AD-A056 468 ARMY ARMAMENT RESEARCH AND DEVELOPMENT COMMAND ABERD--ETC F/G 20/4
METHOD TO EXPERIMENTALLY DETERMINE THE AERODYNAMIC PRESSURE DIS--ETC(U)
JUN 78 M C MILLER

UNCLASSIFIED NL

| OF |
AD
A056468

END
DATE
FILMED
8 -78
DDC

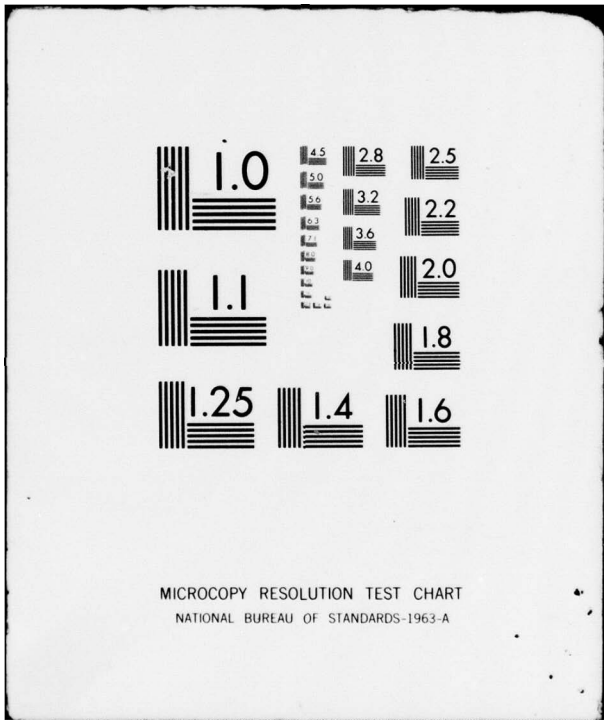
1.0
1.1
1.25
1.4
1.6
1.8
2.0
2.2
2.5
2.8
3.2
3.6
4.0
4.5
5.0
5.6
6.3
MICROCOPY RESOLUTION TEST CHART
NATIONAL BUREAU OF STANDARDS-1963-A

MILLER

LEVEL II

(11) Jun 78 (12) 15p.

(6) JUN 1978

METHOD TO EXPERIMENTALLY DETERMINE THE AERODYNAMIC PRESSURE DISTRIBUTION ON SPINNING BODIES

(10) Miles C. Miller
Weapon Systems Concepts Team
US Army Armament Research and Development Command
Aberdeen Proving Ground, Maryland 21010

PREFACE

This study was supported by combined funding from DARCOM Ballistic Technology and ARRADCOM Chemical Systems Laboratory ILIR programs. The work was conducted between October 1974 and October 1977.

INTRODUCTION

Many Army weapon systems involve spinning aerodynamic bodies such as artillery shells, guided missiles, and Magnus rotor submunitions. The source of numerous flight instability problems has been related to the effect of body spin on the aerodynamic surface pressures. Although wind tunnel testing is the major means for determining the aerodynamic characteristics of these configurations, measurement of the surface pressures has been limited to non-spinning models. This paper describes a new and unique method to experimentally measure the aerodynamic pressure distribution on the surface of spinning wind tunnel models incorporating a special instrumentation scheme. A pressure tap located in the non-spinning inner portion of the wind tunnel model detects the surface pressure through a series of vent holes in the spinning outer portion of the model, the pressure being retained for measurement by means of a sliding seal arrangement. The feasibility of the method was thoroughly demonstrated by means of wind tunnel tests of fundamental model configurations.

The test program was conducted in two phases. ~~First,~~ the test method measured the surface pressure distribution acting on a spinning smooth surfaced cylinder in crossflow in the critical Reynolds number regime. This proved the method's capability to measure a steady state flow condition under various spin rate and free stream velocity conditions. The second phase involved surface pressure measurements on a spinning Magnus rotor. This extended the capability of the testing method to bodies

having irregular surface features and an unsteady, periodic flow field as compared to the smooth surfaced cylinder. Aerodynamic forces and flow field observations obtained by conventional testing techniques confirmed the validity of this unusual method for determining the pressure distribution on spinning bodies.

SYMBOLS

b	span of model; b = 8.482 in
C_D	drag coefficient ($D/q_\infty S$)
C_L	lift coefficient ($L/q_\infty S$)
C_P	pressure coefficient ($\Delta P/q_\infty$)
D	drag force
d	diameter of model; d = 5.171 in
L	lift force
P	pressure on surface of model
P_∞	free stream static pressure
q_∞	dynamic pressure ($\rho_\infty V_\infty^2/2$)
R_d	Reynolds number ($V_\infty d/\nu$)
S	reference area (bd); S = .3046 ft^2
t	time (t = 0 when outer flat surface of upper driving vane is parallel to free stream velocity)
V_∞	free stream velocity
ΔP	surface pressure referred to free stream static pressure ($P - P_\infty$)
α	angle of attack
ρ_∞	air density
ν	kinematic viscosity
$\emptyset$	circumferencial location on model at which pressure is being measured (angle between radial direction of pressure tap and free stream velocity)
Ψ	model rotational attitude (angle between flat external surface of upper driving vane and free stream velocity)
Ω	revolutions of model from t = 0 condition
ω	spin rate
Ω	tip speed ratio ($\omega d/2V_\infty$)

BACKGROUND

A non-spinning body travelling through air causes changes in the local air flow direction and velocity, producing an aerodynamic pressure distribution over the external surface of the body. This surface pressure results in net aerodynamic forces which influence the flight motion and trajectory of the body and represents the important middle stage between the flow field and the resultant aerodynamic forces as illustrated in Figure 1.

In similar manner, a spinning projectile also creates aerodynamic surface pressures which have led to the so-called Magnus effect. This aerodynamic phenomenon, due to the combination of body spin and attitude, produces forces and associated moments which have resulted in flight instability problems for several military projectiles (Ref 1). An understanding of the surface pressure distribution on spinning bodies could lead to identification of the source of the Magnus effect and body configurational modifications for its elimination.

Numerous unsuccessful attempts have been made to measure these Magnus associated pressures in wind tunnel tests utilizing a variety of techniques and instrumentation. The results described in this paper represent the first time that the aerodynamic surface pressure distribution on a spinning body has been obtained experimentally and validated by comparison with direct force measurements.

GENERAL APPROACH

The testing method evolved in this study is based on a unique model design and instrumentation arrangement. The model is composed of two parts: a non-spinning inner portion containing the pressure measuring instrumentation and a spinning outer portion representing the external aerodynamic surface of the body being evaluated. Figure 2 contains a schematic drawing of a cross-sectional view of the wind tunnel model looking along the longitudinal axis (i.e., spin axis) and illustrates the key elements of the test methodology. The stationary (i.e., non-spinning) model core contains a pressure tap oriented radially outward at an angle (Ø) to the direction of the free stream velocity. The angle (Ø) defines the circumferential location on the surface of the model at which the pressure is being measured. A thin walled, cylindrical shell is located concentrically around the core and is attached to the core by means of bearings located at each end. The shell is free to rotate or spin about the core and represents the external surface of the spinning model body. A small vent hole is located through the shell, such that it will line up with the face of the pressure tap once every revolution of the shell about the core. The gap between the face of the pressure tap and the inner surface of the shell is isolated (i.e., longitudinally and circumferentially) by means of a sliding seal attached to the outer end of the pressure tap. The cavity created within this seal will be open to the pressure acting

on the outside surface of the shell when the vent hole is aligned with the tap. When the vent hole rotates past the aligned position, the seal will cause the cavity to retain this pressure. Since the vent hole will be aligned with the cavity for a short time during each revolution, several revolutions of the spinning shell are required to have the pressure in the cavity reach a constant value equal to that acting on the surface of the shell. Tubing from the tap is routed through the model core to a pressure transducer and associated instrumentation located outside of the tunnel. Pressure measurements at various circumferential locations on the surface of the spinning body can be obtained by positioning the core and the attached tap at different attitudes (Ø) to the air flow.

MODEL DESCRIPTION

Details of the smooth cylinder wind tunnel model are shown in Figure 3. Circular end plates were located at each end of the cylinder to reduce tip flow effects. All of the pressure measuring elements in the model were contained within a radial hole located at the core midspan. References 2 and 3 describe the engineering design details associated with the model. The rubber "o" ring represents the most important element of the system in that it established the seal between the pressure tap cavity and the rotating cylindrical shell. Small coil springs pressed the "o" ring against the inner surface of the shell to affect a tight seal. An internal mechanism continuously deposited silicone grease onto the inner shell surface, for sealing and lubrication.

TEST ARRANGEMENT AND INSTRUMENTATION

The wind tunnel tests were conducted in the ARRADCOM Weapon Systems Concepts Team 28 x 40 inch open circuit, continuous flow subsonic wind tunnel. Figure 4 shows the model installed in the tunnel test section. A schematic of the instrumentation arrangement used in the wind tunnel tests is included in Figure 5. The model was mounted in the tunnel such that the longitudinal (i.e., spin axis) was in a vertical attitude and normal to the free stream velocity. Model spin was achieved by means of an electric motor mounted on top of the wind tunnel with a drive shaft extending to the top of the model. Model spin rate was indicated by a magnetic tachometer. The model core support strut was mounted to the tunnel turntable which could be rotated through 360 degrees, allowing the pressure tap to be set at any angle to the flow. The pressure in the cavity was transmitted by plastic tubing routed down the support strut to a transducer located outside the tunnel. The reference free stream static pressure was obtained by a static pressure probe in the tunnel test section. Both transducer and tachometer outputs were indicated as a function of time on a strip chart recorder.

TEST PROCEDURE AND DATA REDUCTION

The test procedure was to establish the desired air flow velocity in the tunnel test section and then use the spin motor to bring the model shell to the test spin rate value. Approximately 30 seconds were required for the pressure reading to equilibrate and be recorded. The core was then rotated to the next angular position while the model was spinning, this sequence being repeated at 10 degree increments around the entire circumference of the model surface. The pressure measurements were reduced to coefficient form and presented graphically. Data reduction techniques and associated equations are fully described in Reference 2. The pressure distribution was integrated over the surface of the model to obtain the resultant lift and drag coefficients as defined in Figure 6.

SMOOTH CYLINDER TEST RESULTS

Pressure distributions were obtained on the smooth cylinder model at various spin rates for three different tunnel velocities corresponding to subcritical, critical, and supercritical Reynolds numbers. The drag coefficient of the non-spinning cylinder in cross flow undergoes an abrupt change between a Reynolds number of 300,000 to 500,000, referred to as the critical Reynolds number regime. Figure 7 shows the drag coefficients as a function of free stream velocity for the non-spinning cylinder with end plates used in these tests. Note that the critical Reynolds number occurs at a tunnel velocity of 90 mph. Test velocities of 60 mph and 120 mph were selected as representative subcritical and supercritical test conditions, respectively.

Figure 8 contains a summary of the pressure distributions obtained during these tests. Note that at certain spin rates, the net lift force has an upward (positive) directional sense. For other spin and velocity conditions it is directed downward (negative). These pressure profiles provide a quantitative measure of the Magnus force and allow interpretation of boundary layer and flow separation effects. A detailed analysis of the pressure data obtained in this study can be found in Reference 2. The relation between the boundary layer, tip speed ratio, and Reynolds number on the resultant aerodynamic forces acting on a spinning cylinder under these flow conditions have been described qualitatively by other investigators (Ref 4). However, the data in Figure 8 is the first time that surface pressure distribution verification of these effects have been experimentally obtained.

A separate series of wind tunnel tests were conducted where the lift and drag forces acting on the model were measured directly by a force balance apparatus. These tests involved the same model and tunnel facility as the pressure measurement tests. Force coefficient values obtained by integrating the measured pressure profile data are shown in Figure 9. The close correlation between the conventionally obtained force data and

the integrated pressure measurements from this new testing method validates the pressure measurement method for this smooth model, steady flow situation. Further, the primary benefit of this method is the detailed insight into the source of the resultant forces provided by the pressure distribution data.

MAGNUS ROTOR TESTS

A Magnus rotor is an asymmetrically shaped body that, when placed in an air stream, will autorotorate or spin, producing large aerodynamic lift and drag forces. The Magnus rotor represents an aerodynamic configuration with an irregular external surface as opposed to the smooth surfaced cylinder previously tested. Also, unlike the steady flow field of the smooth cylinder, the Magnus rotor generates an unsteady, periodic flow field. The model used in the previous tests was modified to a cylindrical Magnus rotor configuration by the simple addition of the four full span driving vanes and additional vent holes. This configuration is representative of Magnus rotors and their aerodynamic characteristics.

Figure 10 contains a cross-section view looking along the longitudinal axis of the Magnus rotor wind tunnel model. Because of the irregular external features, the surface pressure was measured at nine specific locations relative to the external features. Due to the 90 degree rotational symmetry, the model only required vent holes over a single quadrant. Vent holes 8, 7, 6, 5, and 1 extended radially through the shell thickness of .125 inches. Vent holes 5, 4, 3, and 2 had to pass through the thickness of the driving vane resulting in a longer vent hole path, the longest being vent hole 5 with a total length of .625 inch. This relatively long length did not interfere with the ability to accurately acquire the surface pressure.

The wind tunnel facility, model mounting, and instrumentation arrangement were identical to that used with the smooth cylinder. The model was spun by means of the spin motor to 2050 RPM providing the desired 0.46 steady state tip speed ratio for the tunnel velocity of 100.5 FPS. Only one vent hole at a time was open for a specific test, the others being closed off. The testing procedure was similar to that of the smooth cylinder, with pressure data being obtained at 10 degree increments over the entire circumference of the model surface.

Figure 11 contains selected examples of pressure data for three of the vent hole locations. These data indicate the pressure acting at that particular location on the surface of the model over a complete 360 degree rotation relative to the free stream direction. Similar plots were obtained for all vent hole locations. At a specific rotational attitude of the spinning model a particular vent hole location occurs at four different circumferential positions relative to the free stream vector as shown in Figure 12. Using data for all the vent holes, the complete sur-

face pressure distribution acting over the spinning Magnus rotor can be determined. Figure 13 shows the pressure distribution acting on the spinning Magnus rotor model over a quarter revolution at 11.25 degree increments. Note that for the 2050 RPM spin rate of the model, this corresponds to the pressure distribution at 0.9 milli-second intervals. This cycle is repeated four times during a complete 360 degree revolution. Once the basic data plots are obtained, pressure distributions can be determined over any time increment.

The resultant lift and drag coefficient were computed by integrating the pressure distribution over the model surface. These values are shown in Figure 13 and are presented as a function of model rotational attitude and time in Figure 14. Although the cyclic nature of the lift and drag of a Magnus rotor had been considered, this represents the first time that quantitative data have been obtained. Note that both the lift and drag are sinusoidal and out of phase. Because of the high rotational spin rates of Magnus rotors and the limited response of wind tunnel balance systems only the average aerodynamic forces can be measured in force type wind tunnel tests. The values for both the lift and drag derived from the pressure data show good correlation with the average values directly measured during separate force wind tunnel tests as also shown in Figure 14. The integrated pressure data, however, provide a more detailed insight into this cyclic aerodynamic effect. Complete details of the Magnus rotor tests are contained in Reference 5.

Flow visualization tests were conducted with the cylindrical Magnus rotor using a special smoke flow wind tunnel facility. High speed film records obtained from these tests were used to construct line drawings of the flow field streamlines for selected model rotational attitudes. Figure 15 shows these streamlines superimposed on the pressure distribution measured for the same conditions, providing a complete physical picture of the flow field, aerodynamic surface pressure distribution, and resultant aerodynamic forces for the spinning Magnus rotor at sequential instants of time. The unsteady, separated flow and in particular, the strong vortex shed off the retreating (upper) driving vane are graphically depicted. Note that this vortex produces a high velocity flow and corresponding low pressure over the forward portion of the vane. This figure illustrates the powerful tool provided by the pressure distribution toward interpreting and analyzing aerodynamic phenomenon on spinning configurations.

The flow over the Magnus rotor although unsteady, is periodic with model rotation. It is this latter factor that allows this pressure measuring method, which uses steady state instrumentation, to measure an unsteady flow condition. This same situation occurs in most non-transient flow fields around spinning bodies, thereby allowing this testing method to be used to investigate a variety of aerodynamic problems.

FUTURE APPLICATIONS

The spinning body in cross flow represents an especially demanding condition for demonstrating the pressure measuring capabilities of this test method due to the severe influence of Reynolds number and model spin effects in the case of the smooth cylinder and the unsteady vortex flow for the Magnus rotor. The successful results indicate that the test method can be applied to a variety of model configurations and model orientations to the air flow (i.e., angles of attack). Because all of the instrumentation elements are internal to the model, the method could also be used in any Mach number regime including subsonic, transonic, and supersonic.

As the previous tests with the smooth cylinder will allow extension of the testing method to a variety of spinning models having smooth external shapes, so the Magnus rotor tests allow the method to be used with spinning models having irregular surface features as illustrated in Figure 16. Multiple pressure taps could be incorporated into a wind tunnel model at several locations along its length to provide the pressure distribution acting over the entire model surface. The most important features of this testing method are summarized as follows:

- .All elements of instrumentation located within model or outside tunnel test section
- .No inertial or dynamic loads acting on transducer
- .Direct connection between pressure tap in model and instrumentation outside tunnel
- .Constant pressure reading does not require high response transducer
- .Rapid pressure surveys possible
- .Applicable to any model orientation to free stream
- .Can be used in any speed regime (subsonic, transonic, and supersonic)
- .Will function with models having irregular external surface features
- .Can be used with both steady flow or unsteady, periodic flow situations

CONCLUSIONS

1. This study has demonstrated the validity of a new testing method by which the aerodynamic pressure distribution acting on the surface of a spinning body can be measured in the wind tunnel.

2. Integration of the resulting pressure distribution data not only provides a quantitative measure of the Magnus forces but the pressure distribution provides a unique insight into the critical middle stage between the flow field and the resulting aerodynamic forces allowing a more accurate interpretation of boundary layer and flow separation effects.

3. The test method can be utilized in both steady flow and unsteady periodic flow situations and is applicable to a variety of model external configurations, angles of attack, spin rates, and Mach number regimes.

REFERENCES

1. Jacobson, I. D., "AGARDograph No. 171. Magnus Characteristics of Arbitrary Rotating Bodies." November 1973.

2. Miller, M. C., "A Technique to Measure the Pressure Distribution Acting on the Surface of a Spinning Body in a Wind Tunnel," Edgewood Arsenal Technical Report ED-TR-76070. September 1976. Unclassified.

3. Miller, M. C., "Surface Pressure Measurements on a Spinning Wind Tunnel Model," AIAA Journal, Page 1669. December 1976.

4. Swanson, W. M., "The Magnus Effect: A Summary of Investigations to Date," Journal of Basic Engineering. Transactions of the ASME, Pages 461-470. September 1961. Unclassified.

5. Miller, M. C., "Wind Tunnel Measurements of the Surface Pressure Distribution on a Spinning Magnus Rotor," Proceedings AIAA 10th Aerodynamic Testing Conference. 19-21 April 1978.

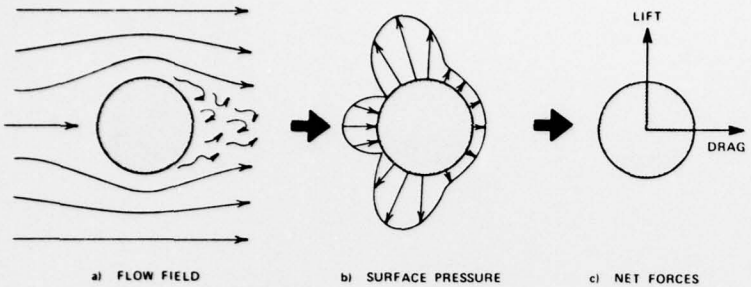

Figure 1. AERODYNAMIC EFFECTS

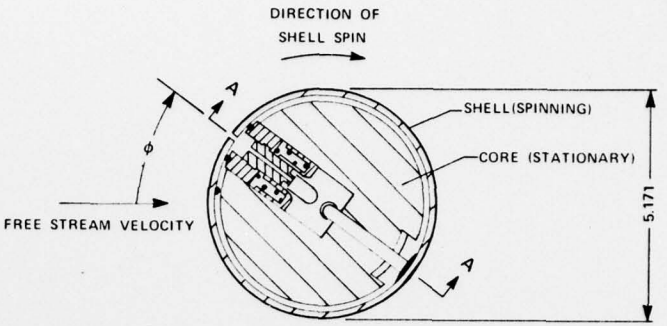

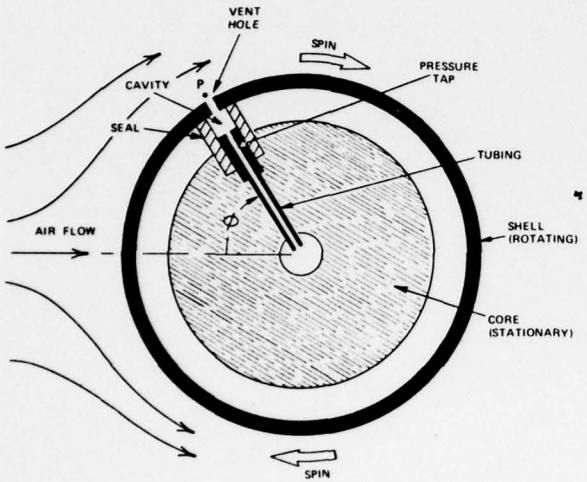

Figure 2. TESTING METHODOLOGY

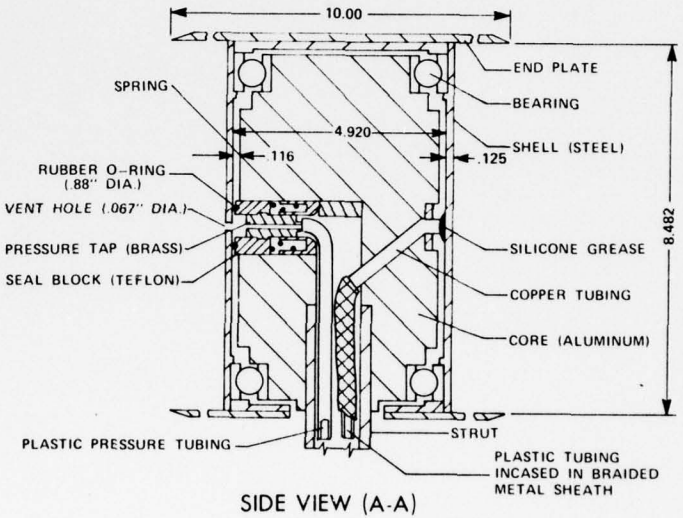

Figure 3. WIND TUNNEL MODEL DETAILS

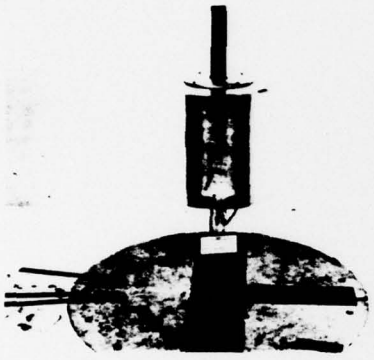

Figure 4. MODEL MOUNTED IN WIND TUNNEL

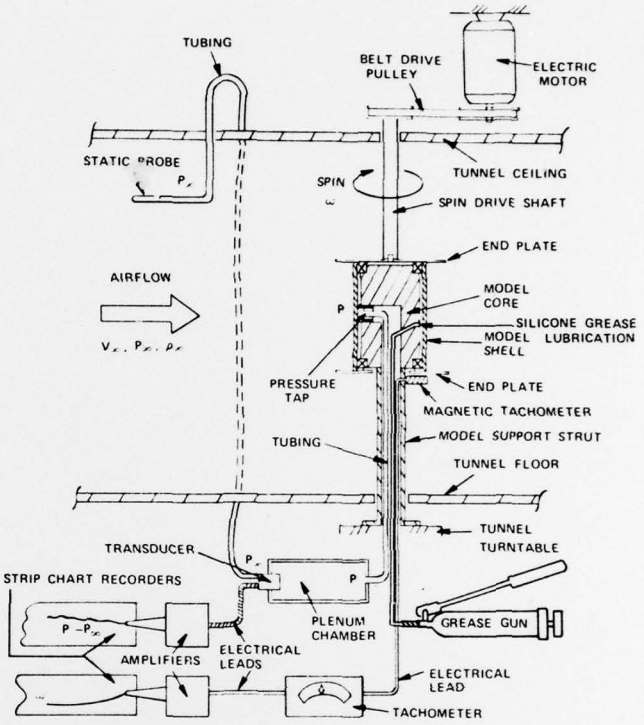

Figure 5. INSTRUMENTATION ARRANGEMENT

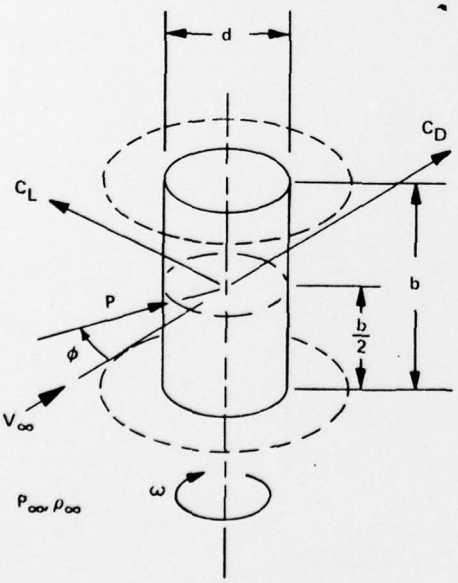

Figure 6. DATA SYMBOLS

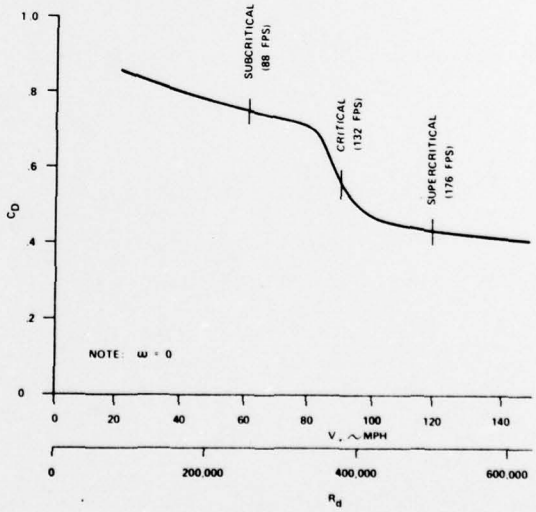

Figure 7. DRAG COEFFICIENT FOR NON-SPINNING SMOOTH CYLINDER MODEL IN CROSS FLOW

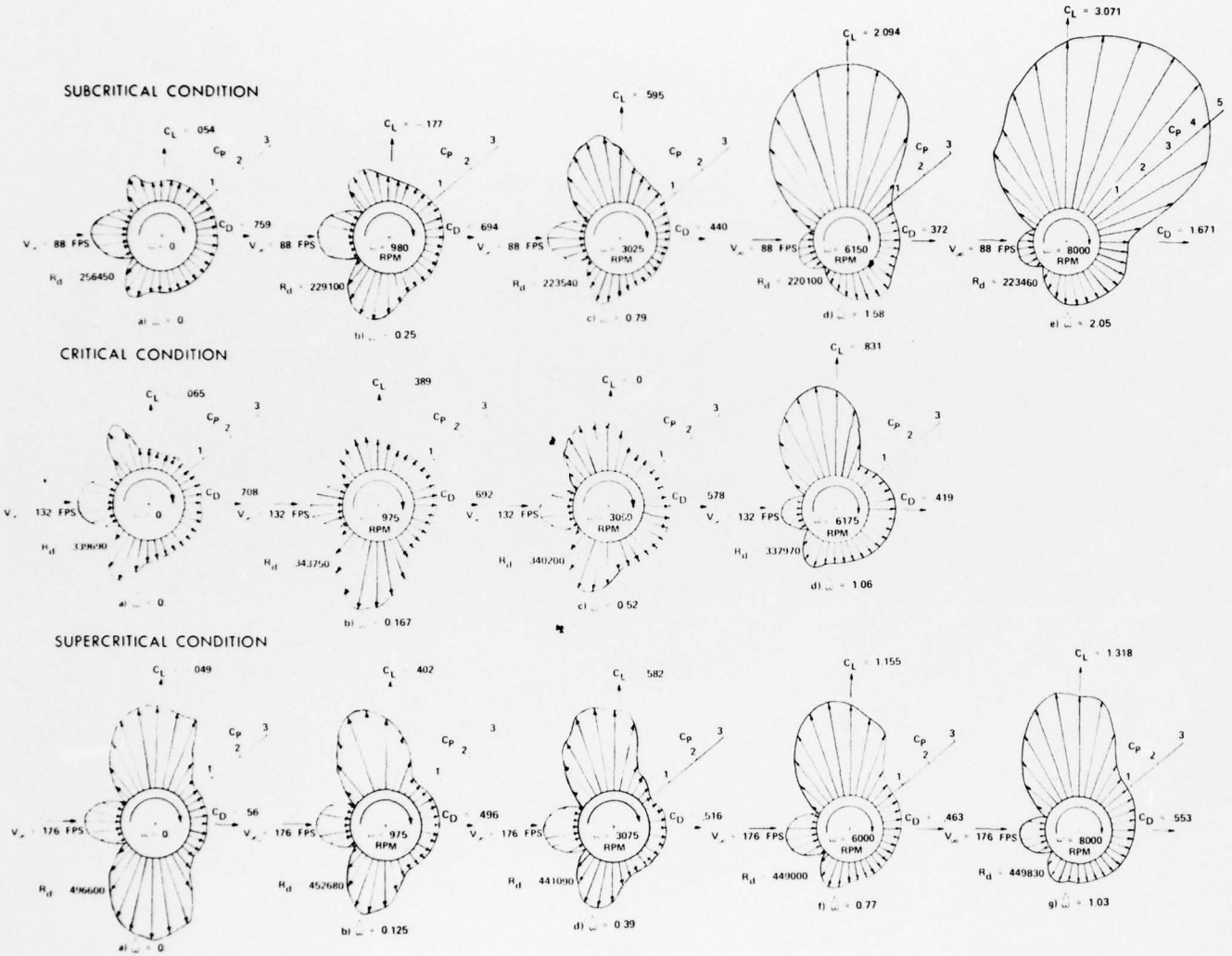

Figure 8. SURFACE PRESSURE DISTRIBUTIONS ON SPINNING SMOOTH CYLINDER IN CROSS FLOW FOR VARIOUS FREE STREAM VELOCITIES AND SPIN RATES

V_∞ (FPS)	ω (RPM)	$\hat{\omega}$	R_d	DATA OBTAINED FROM PRESSURE TESTS C_L	DATA OBTAINED FROM PRESSURE TESTS C_D	DATA OBTAINED FROM FORCE TESTS C_L	DATA OBTAINED FROM FORCE TESTS C_D
88	0	0.	256450	.054	.759	0	.755
	980	.25	229100	.177	.694	.180	.690
	3025	.79	223540	.595	.440	.560	.480
	6150	1.58	220100	2.094	.372	2.20	.620
	8000	2.05	223460	3.071	1.671	3.60	1.80
132	0	0.	339690	.065	.708	0.	.700
	975	.167	343750	.389	.692	.530	.560
	3050	.520	340200	0.	.578	.06	.530
	6175	1.06	337970	.831	.419	1.11	.425
176	0	0.	496600	.049	.560	0	.440
	975	.125	452680	.402	.496	.240	.480
	3075	.390	441090	.582	.516	.58	.510
	6000	.77	449000	1.155	.463	.73	.460
	8000	1.03	449830	1.318	.553	1.510	.600

NOTE: FORCE DATA ONLY OBTAINED UP TO 4500 RPM. COMPARISON OF DATA ABOVE THIS SPIN RATE IS BY EXTRAPOLATION.

Figure 9. COMPARISON OF FORCE AND PRESSURE TEST DATA

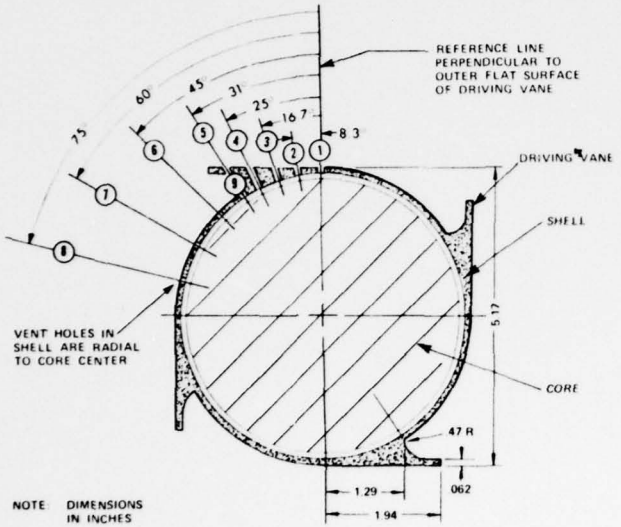

Figure 10. MAGNUS ROTOR MODEL CONFIGURATION

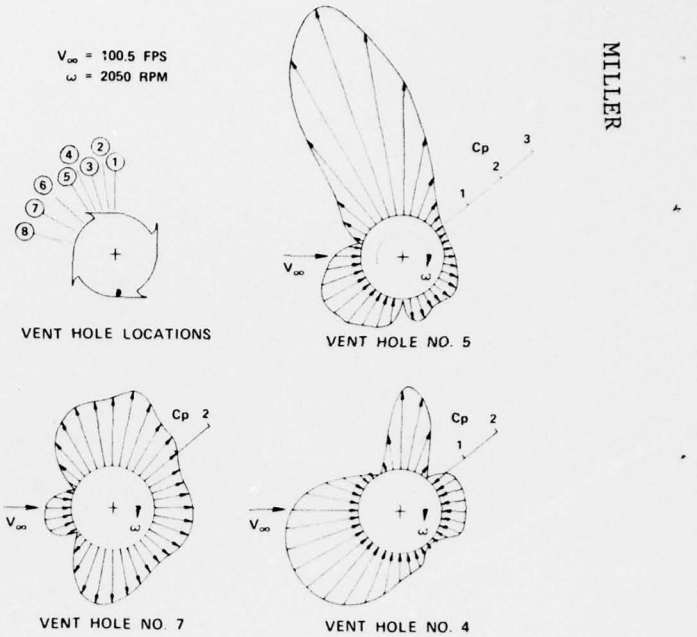

Figure 11. SURFACE PRESSURE DURING A COMPLETE MODEL REVOLUTION

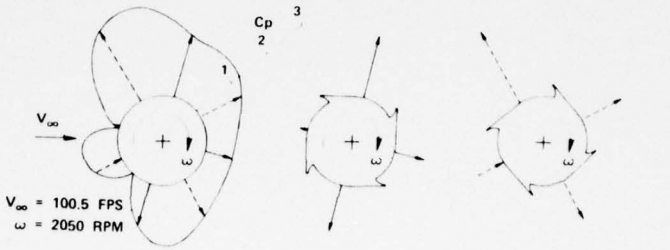

a) PRESSURE AT VENT HOLE NO. 8 DURING A COMPLETE MODEL REVOLUTION

b) PRESSURES AT VENT HOLE NO. 8 AT A MODEL ROTATIONAL ATTITUDE OF $\psi = 0^o$

c) PRESSURES AT VENT HOLE NO. 8 AT A MODEL ROTATIONAL ATTITUDE OF $\psi = 45^o$

Figure 12. PRESSURE DETERMINATION

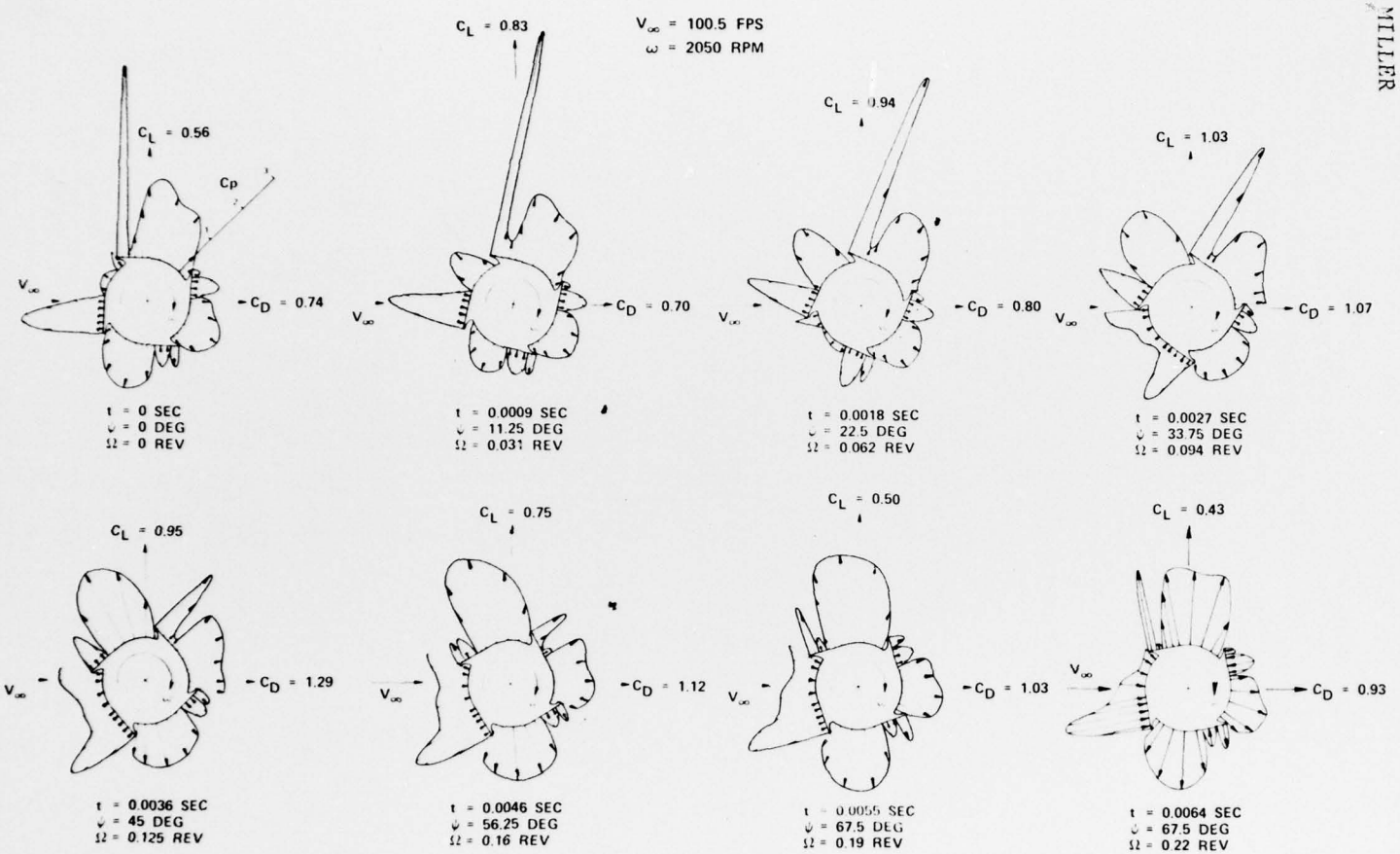

Figure 13. SURFACE PRESSURE DISTRIBUTION ON SPINNING MAGNUS ROTOR IN CROSS FLOW AT SPECIFIC TIME INTERVALS

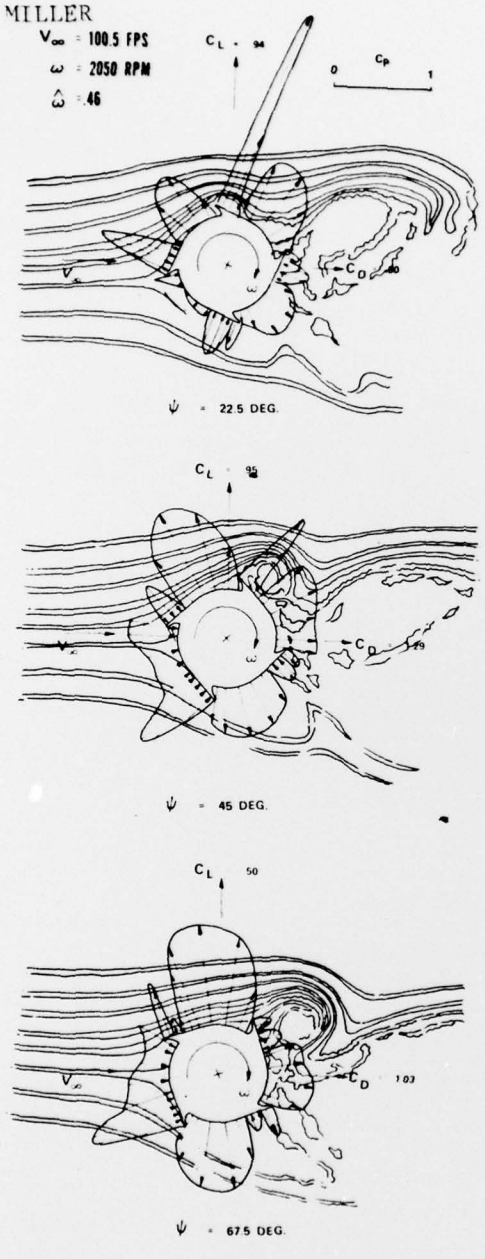

Figure 15. FLOW FIELD, SURFACE PRESSURE DISTRIBUTION, AND RESULTANT AERODYNAMIC FORCES ON SPINNING MAGNUS ROTOR AT VARIOUS ROTATIONAL ATTITUDES

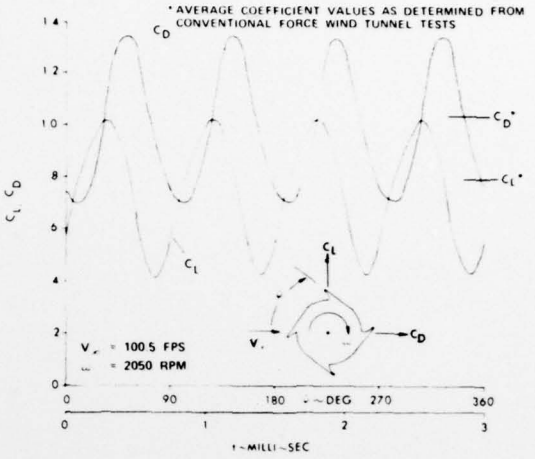

Figure 14. LIFT AND DRAG COEFFICIENT AS A FUNCTION OF TIME FOR SPINNING MAGNUS ROTOR

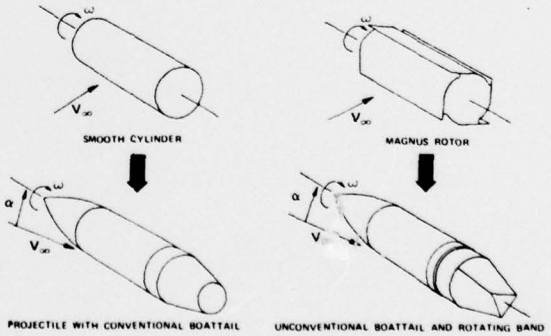

Figure 16. FUTURE APPLICATIONS FOR SURFACE PRESSURE TESTING METHOD